



# Preserving microstructure of concrete under load using the Wood's metal technique

K.M. Nemati\*

*Departments of Construction Management/Civil Engineering, University of Washington, Seattle, Washington, 98195-1610, USA*

Accepted 7 October 1999

## Abstract

A special experimental technique was developed which made possible the preservation of microstructure and the compressive stress-induced microcracks in concrete as they exist under applied loads. Cylindrical specimens of concrete were tested under uniaxial and triaxial compression. The resulting induced cracks were impregnated with a metal alloy, Wood's metal, that liquefies at higher temperatures (70–85°C), but is solid at normal temperatures. At the stress of interest, this alloy was solidified to preserve the stress-induced microcracks as they exist under load. Scanning Electron Microscopy (SEM) was employed to capture images from the cross sections of the concrete specimens. Stereology presents the geometrical statistical background for relating three-dimensional structures to their two-dimensional sections. Stereological estimates were obtained for total crack extension per unit of volume. Further, two-dimensional features of the cracks were analyzed in the section plane, such as orientation distribution, and length. © 2000 Elsevier Science Ltd. All rights reserved.

## 1. Introduction

Concrete is a heterogeneous, multiphase material. On a macroscopic scale it is a mixture of cement paste and fine and coarse aggregates, with a range of sizes and shapes. With regard to its mechanical behavior, concrete is often considered to be a three-phase composite structure, consisting of aggregate particles, the cement paste matrix in which they are dispersed, and the interfacial transition zones around the aggregate particles.

Since the 1920s, researchers have suggested and assumed the existence of different kinds of defects called microcracks that would occur in concrete. However, only since the early 1960s have such cracks been observed, measured, and characterized in the interior of the system [1]. In the 1970s and 1980s the development of nonlinear fracture mechanics models enabled the structure and behavior of concrete to be taken into

account. In the 1980s and 1990s, further research has led to the increasingly common application of fracture mechanics in the design of beams, anchorage, and large dams. In spite of this, the theory of fracture mechanics in concrete is not yet as mature as continuum theories, such as elasticity, viscoelasticity, and thermal problems. This is in part due to the limited understanding of the formation and propagation of microcracks in concrete. Early stereological approaches to analyzing damage evolution in concrete date back to the 1970s [2–4]. Such studies were able to reveal mechanisms of damage evolution in complicated loading cases, such as in the low-cycle fatigue domain [5]. By application of the fractal concept, recently the influence could be assessed of the sensitivity of the quantitative image analysis of microcracking in concrete on the spatial morphological features [6,7].

## 2. Methods for studying microcracking

The investigation of microcracking ranges from a macroscopic study of the behavior of cracked speci-

\* Tel.: +1-206-685-4439; fax: +1-206-685-1976.

E-mail address: nemati@u.washington.edu (K.M. Nemati).

mens to a microscopic study of the cracks themselves. The presence of microcracks was predicted on the basis of macrobehavior and verified by microscopic studies.

Several methods have been used to study the microcracking of concrete. These include acoustic emission, sonic testing, dye technique, hydrophilic tracer liquid technique, mercury intrusion porosimetry, X-ray technique, optical and electron microscopy computerized tomography analysis, holographic interferometry, fluorescent spraying technique [2,4], confocal microscopy [8], and other techniques to examine fracture networks and cracks [9–13]. Some of these techniques are limited in their resolution, their sensitivity in detecting cracks, or their ability to make observations over a large area. Other methods are incapable of examining the specimen while under load or they require special preparation of the specimen, which alters its behavior.

The method described here involves the application of a metal, Wood's metal, in the liquid phase, which preserves the microstructure under load of stress-induced microcracks in concrete. It has been used in

the past few years to study the microstructure of different materials. It was employed for porosimetry and to measure the contact area and void space between the surfaces of natural fractures [14], the fracture of rocks [15], to fill voids and microcracks in clastic rock specimens during loading, and solidifying it before unloading to preserve the microstructure in specimens under load [16], and to study the generation and interactions of compressive stress-induced microcracks in concrete and marble [17,18]. Wood's metal is a fusible alloy, which has a melting range from 71°C to 88°C and is solid at room temperature. It has a Young's modulus of 9.7 GPa, a density of 9.4 g/cm<sup>3</sup> [14], and goes through minimal volume change during hardening (it has thermal expansion of 10<sup>-6</sup> in/in). In the liquid phase it is nonwetting, with an effective surface tension of about 400 mN/m and can penetrate into flat cracks with apertures as fine as 0.08 microns under a pore pressure of 10 MPa. The specimens were subjected to compressive loading of about 80–85% of their ultimate strength ( $f'_c = 11,000$  psi). The advantage of such an alloy is that it can be intruded into voids and stress-

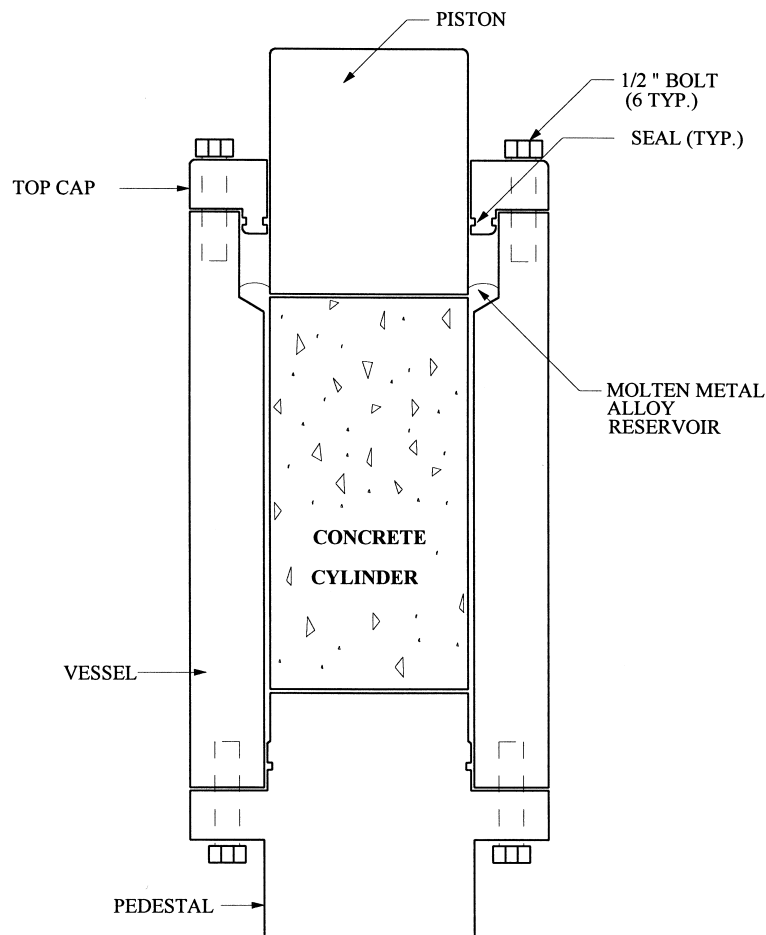


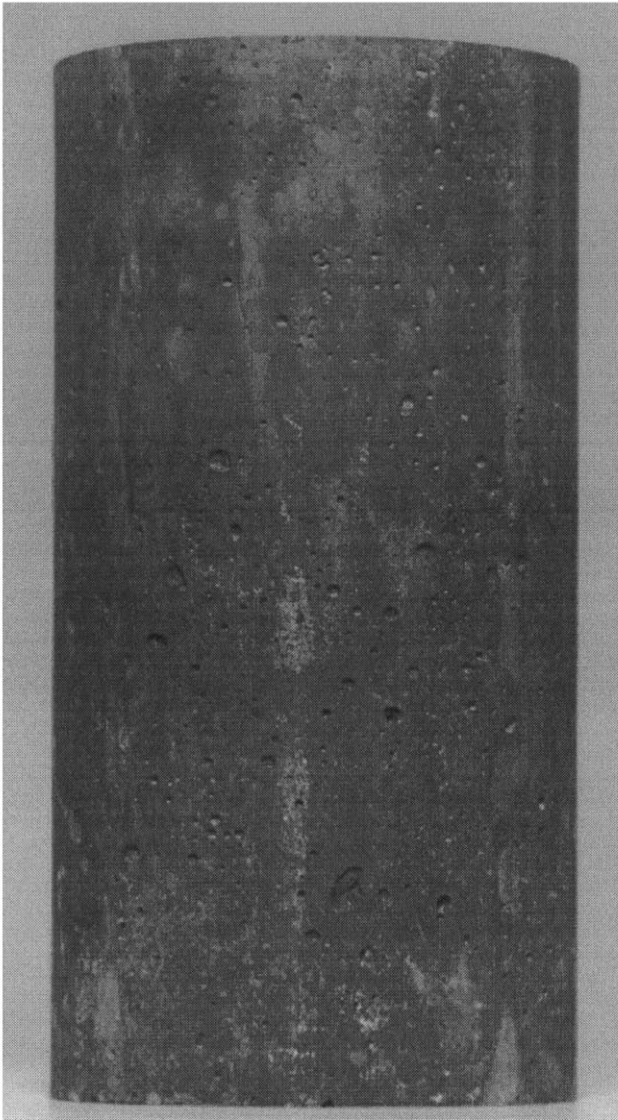
Fig. 1. Test apparatus.

induced microcracks while the specimen is held at the desired stress level and then solidified to preserve the geometry of the microcracks induced. Figs. 1 and 2 show the schematic test setup and unconfined and confined specimens. The confining stress used to generate triaxial compression was supplied by stainless steel wires that were wound around the concrete cylinders at a pre-tension of 150 lbf.

The experimental technique used in conjunction with scanning electron microscopy (SEM) with backscattered electrons (BSE), allows the detailed observation of microcracks in concrete as they exist under load. The SEM was operated at 15 kV and a probe current of around 1 nA at a working distance of 15 mm. The images were acquired by the image analyzer at a mag-

nification of  $\times 60$  and digitized into an array of  $512 \times 512$  pixels, with 256 gray levels (1 pixel =  $3.3 \mu\text{m}$ ). A typical BSE image is given in Fig. 3. Figure 4 shows a histogram of the distribution of gray levels in the BSE image superimposed on the original image. As the average atomic number of the Wood's metal is much higher than those of the cement paste and the aggregates, impregnated cracks and pores can be easily distinguished in the BSE image. This technique also avoids the problem of crack formation during specimen preparation. The peak at the right (high gray level) corresponds to the areas of Wood's metal, while the peaks to the left correspond to the cementitious phases and aggregate. This histogram was used to select the threshold value for discriminating the areas

(a)



(b)

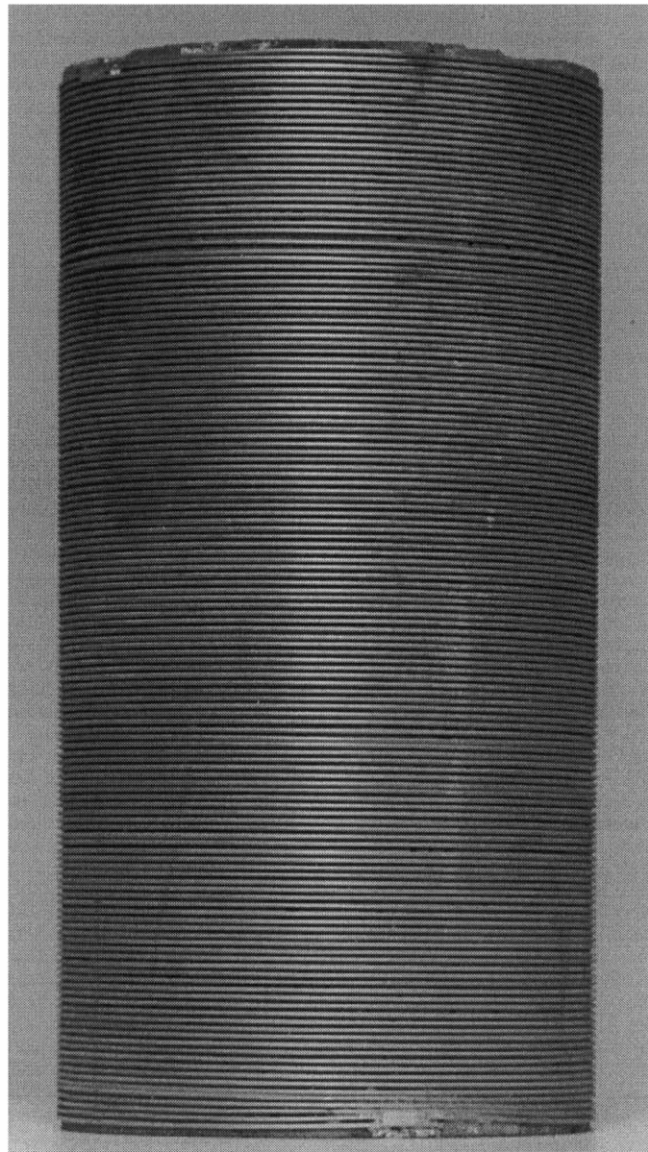


Fig. 2. Unconfined and confined samples.

of Wood's metal. The resulting image (Fig. 5) included small isolated pores, which were eliminated by the application of a minimum size threshold (scrap) for objects of 10 pixels (minimum feature size of approximately 33  $\mu\text{m}$ ).

Next, a skeletonized binary image was obtained by binary thinning. For every thinning step, pixels that were not relevant to the connectivity of an object were removed from the object margins, i.e., converted into background pixels, thus connectivity of objects is maintained. This process was continued until all objects were reduced to a width of one pixel that approximates the skeleton. Fig. 6 is the final binary image used for stereological measurements.

### 3. Stereology

All matter can be described in terms of zero, one, two, and three dimensions. Stereology deals with the interpretation of three-dimensional structures by means of their two-dimensional sections or projections.

In a way, stereology is the opposite of photogrammetry, which utilizes three-dimensional images in order to construct flat maps. Techniques conventionally used for studying the three-dimensional structure of materials, particularly in other material sciences, are often stereological ones. Stereology encompasses numerical characterizations of geometrical aspects of those features of the microstructure of interest, like microcracks in concrete. In its broadest context, stereology includes all aspects of the methodology for a quantitative study of spatial structures, i.e., the design of the experiments, the sampling strategy, the pattern recognition and the quantitative image analysis operations, the geometrical statistical theoretical framework for 3-D estimation of spatial parameters and their accuracy, and the qualitative interpretation of the outcomes.

There are various stereological strategies for solving spatial problems. The major distinction is coming from the objects of interest. This can be single objects, of which the internal structure can be analyzed by means of a serial sectioning approach. This requires a deterministic strategy for 3-D reconstruction. In materials

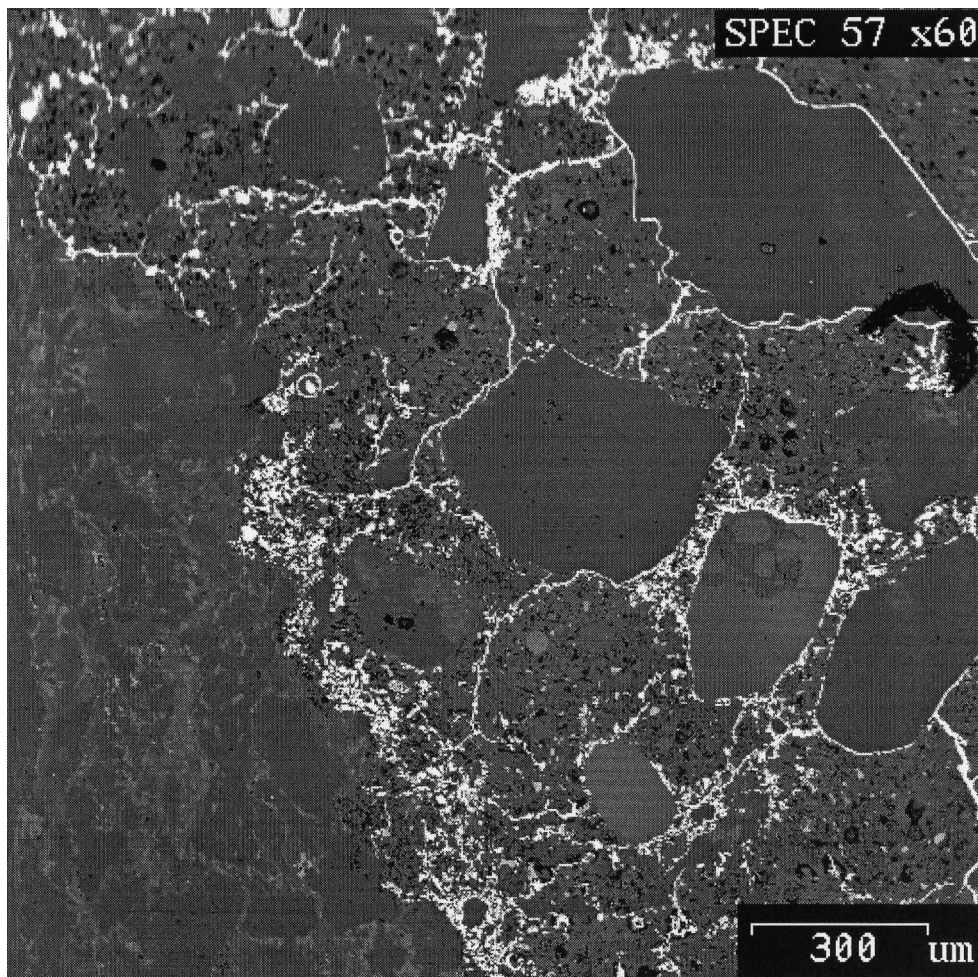


Fig. 3. A typical BSE image.

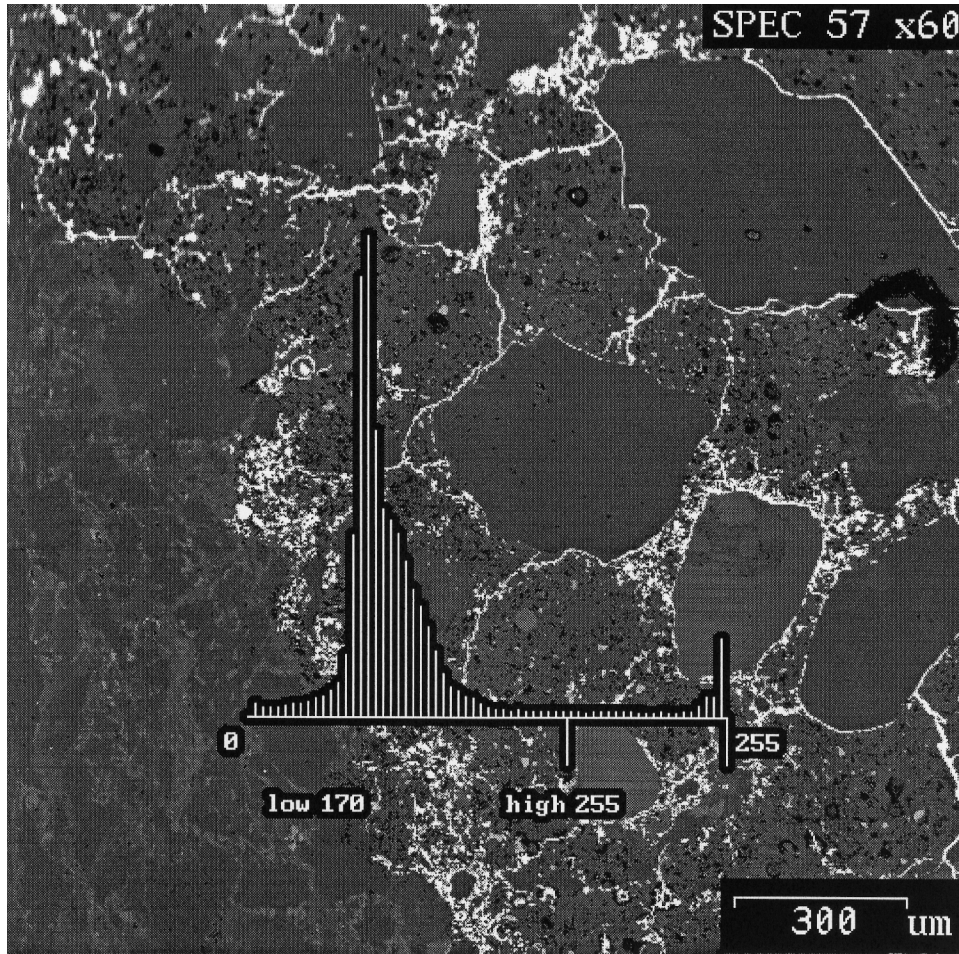


Fig. 4. The gray level histogram.

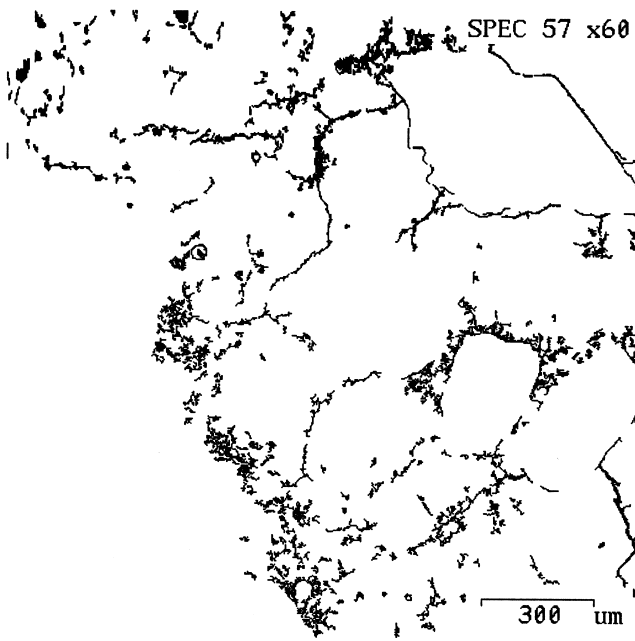


Fig. 5. Thresholded image.

science, however, the common field of interest is the assessment of global spatial parameters of a dispersed ‘particulate’ phase. Note that ‘particulate’ can be interpreted in terms of aggregate particles of macroscopical dimensions, or of cement particles on microlevel. Pores or other defects are obtained upon taking zero phase stiffness. In such cases of dispersed elements like cracks in the material body, stereological approaches are based on statistico-geometrical methods, encompassing sometimes a large number of two-dimensional images. It is the approach utilized in this study.

Reliable prediction of 3-D features of the structure of interest, in the present case of cracks in a loaded specimen, can only be achieved when based on a representative sample. In general, this implies a sample of random sections or projections of sufficient extent. Basically, the quality of the prediction is inversely proportional to the square root of the effort. So, taking the sample four times larger will improve the quality of the estimate by a factor two. Only in exceptional cases, the structure itself consists of randomly dispersed elements. In such cases, a single section, if extensive enough to contain a statistically significant

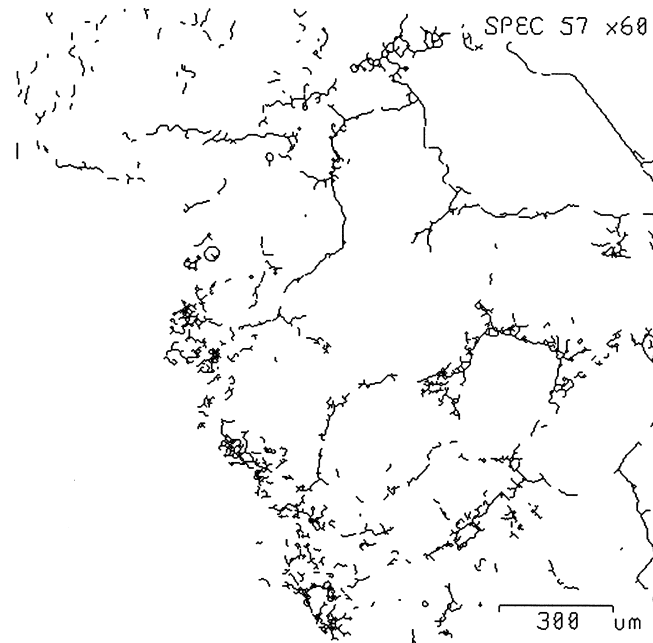


Fig. 6. Binary-thinned image of the crack network in concrete.

number of features, will suffice to obtain valid results. Fundamental expressions have been determined which relate measurements on two-dimensional sections to the three-dimensional structure. Table 1 presents some of the symbols commonly used relevant to this work.

The relationships between  $L_A$  and  $S_V$  with  $P_L$  (Table 1) are presented as follows [19].

(Crack) surface area per unit volume,  $S_V$ :

$$S_V = 2P_L \mu\text{m}^2/\mu\text{m}^3 \quad (1)$$

(Crack) length per unit area,  $L_A$ :

$$L_A = \left(\frac{\pi}{2}\right)P_L \mu\text{m}/\mu\text{m}^2 \quad (2)$$

and combined

$$\frac{\pi}{2}P_L = L_A = \frac{\pi}{4}S_V \quad (3)$$

#### 4. Application of stereology to concrete fracture

Stroeven [20–23], Ringot [24], and Massat et al. [25] successfully applied the concept of stereology to study micromechanical aspects of concrete. With the advent of modern image analysis systems, it is now possible to perform stereological analysis on a great number of images accurately and expeditiously, whereas in the past this was not achievable by means of manual methods.

The present investigation emphasizes the results from concrete cylinders tested in compression with various degrees of lateral confinement. While under load, the specimens were impregnated with Wood's metal to preserve the pre-loading cracks and the stress-induced cracks.

After the metal solidified, sections were cut from the specimens and examined in a scanning electron microscope. Image analysis and stereology were used to characterize the 3-D extent of cracking. Additional objectives were to determine the geometry (shape and

Table 1  
List of basic stereological symbols and their definition

Symbol	Dimensions	Definition
$P_L$	$\mu\text{m}^{-1}$	Number of intersections per unit grid line length between features (i.e., cracks) in the section plane, and a superimposed randomly oriented system of parallel lines
$P_L(\theta)$	$\mu\text{m}^{-1}$	Ibid, but with the line array oriented at an angle (to a reference axis)
$L_A$	$\mu\text{m}/\mu\text{m}^2$	Total crack length in a section per unit of area
$S_V$	$\mu\text{m}^2/\mu\text{m}^3$	Total crack surface area per unit of volume

size) of the stress-induced 2-D microcracks as they exist under load, and to assess the dependence of these damage parameters on types of concrete and on the loading confinement.

The backscatter images obtained from scanning electron microscopy (Fig. 3) were analyzed using a Kontron image analyzer. Computer programs were developed to analyze the images based on the concept of stereology. The binary image (Fig. 6) is then intersected by an array of straight parallel lines at successively increasing angles of 0°, 15°, 30°, 45°, 60°, 75°, 90°, 105°, 120°, 135°, 150°, and 165° (Fig. 7).

The number of crack intersections at a given angle,  $\theta$ , is thereupon determined. Table 2 summarizes the results of the stereological analysis obtained from intersecting the array of straight parallel lines at different angles with the binary images of crack network.

4.1. Orientation of microcracks

Fig. 8 is the plot of the number of intersections of the line array with the network of thinned cracks for successive orientations of the grid based on data from Table 2 and using Eq. (1) (loading direction is  $\theta=0, 180$ )

From Fig. 8 it is apparent that on a microscopic scale, the cracking is relatively isotropic. The uniaxial section reveals some tendency for a higher number of intersections for line arrays oriented parallel to the stress axis, indicating that the cracks in this section tended to run perpendicular to the loading direction. However, this tendency is not present in the sections of the confined specimens.

Any tendency to anisotropy and to anisometry in the underlying damage structure is due to the non-hydrostatic character of the loading. The heterogeneity of concrete greatly affects the details on microlevel of

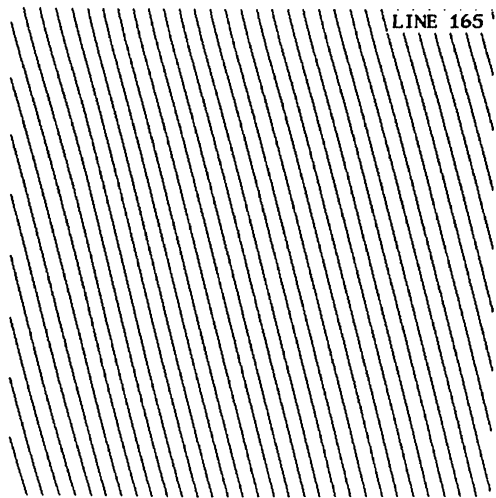


Fig. 7. Array of straight parallel.

Table 2  
Data from stereological analysis

Specimen	Area	% Area	0	15	30	45	60	75	90	105	120	135	150	165	180	Total	$S_V$
No load	5228	0.98	21	20	19	16	18	20	19	19	18	16	18	20	21	226	7.0E-4
Uniaxial	10,829	1.90	43	43	39	35	38	41	39	40	36	34	39	43	43	470	1.5E-3
Confined	6274	1.21	25	25	23	20	22	23	22	22	21	19	23	25	25	269	8.3E-4

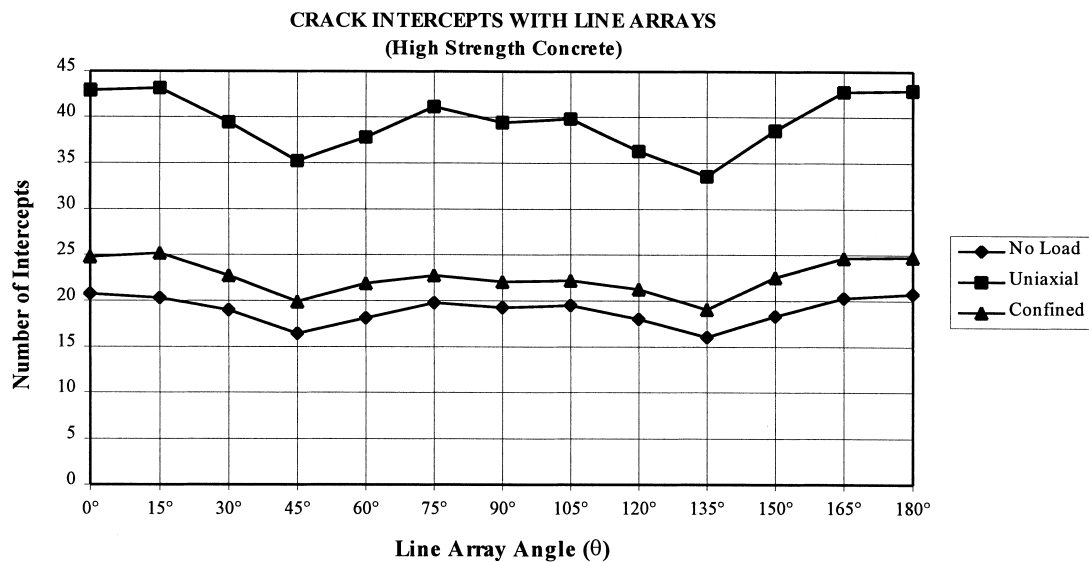


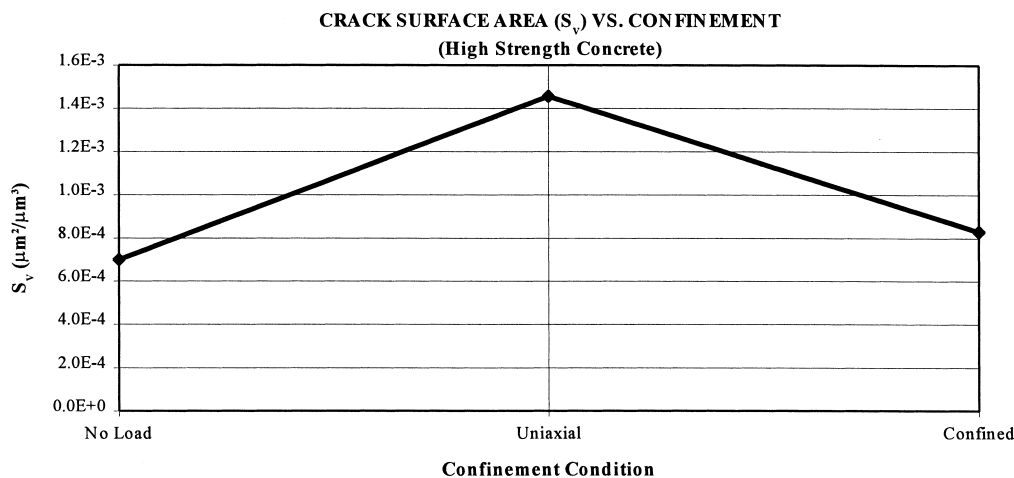
Fig. 8. Areal crack orientation distribution.

damage evolution. The relatively stiff and strong particles play an important role in normal concretes, particularly because of their relative poor bond to the surrounding matrix. Visual examination makes it clear that a large proportion of the cracks occur at the cement paste/aggregate interfaces, like already reported in the 1960s [1]. Although, these interfaces will be randomly oriented, even cracking in the virgin state will never be random. So, the starting point of any mechanical test will involve testing concretes with a partially oriented defect structure. Whether this should be considered significant depends on the goals of the investigations. The same can be said, but to a far lesser extent, for the non-random influence of non-hydrostatic loadings on damage evolution. Total crack sur-

face area per unit of volume — seen as a relevant global 3-D damage evolution parameter — could be assessed with sufficient accuracy for particular purposes, e.g., when comparing influences of significantly different loading regimes, such as in this paper.

#### 4.2. Crack surface area ( $S_V$ )

The stereological measurement of the surface-to-volume ratio,  $S_V$  ( $S/V$ ), was determined from the basic equation for obtaining the total crack surface area per unit of volume. Plots of  $S_V$  as a function of confinement are presented in Fig. 9. Crack surface area,  $S_V$  decreases as the confining stresses increases.

Fig. 9. Crack surface area ( $S_V$ ) as a function of confinement from data in Table 2.

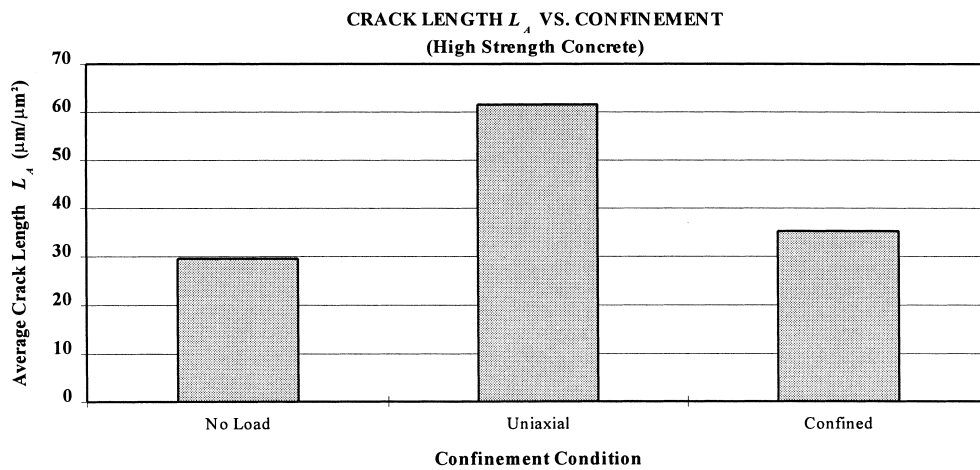


Fig. 10. Stereological measurement of total crack length per unit of area as a function of confinement.

#### 4.3. Crack length distribution

Based on stereological analysis,  $L_A$ , the total crack length per unit area (Eq. (2)) also decreases with increasing confining stresses. Fig. 10 shows the relationship between  $L_A$  and confinement condition.

### 5. Summary and conclusion

The concept of stereology, which deals with the interpretation of three-dimensional structures by means of their two-dimensional sections, was applied to analyze images of concrete specimens subjected to different loading regimes.

Concrete has the inherent quality of being heavily cracked even before a load is applied. When concrete specimens were subjected to compressive loading, microcracks were generated by several different mechanisms and had an orientation that was generally within  $15^\circ$  of the direction of the maximum compression. The stereological prediction of the total surface area per unit of volume of the cracks — or the crack surface density —  $S_V$ , was found to be strongly influenced by the confining stress: the application of the confining stress resulted in a decrease in crack surface density. The reason for this behavior is because the stress intensity factor is a fundamental quantity that governs the stress field near the crack tip. The propagation of microcracks is controlled by the stress intensity factor at the microcrack tips, resulting from both local tensions, which generate the microcracks, and the overall stress field. The confining stress, which is orthogonal to the direction of maximum compression, adds a negative stress intensity factor, inhibiting further propagation of the microcracks.

### Acknowledgements

The author would like to express his appreciation to the late Professor Neville G.W. Cook, Dr Larry R. Myer and Professor Paulo J.M. Monteiro of the University of California at Berkeley for their guidance in designing the test apparatus and for advice on experimental procedures.

### References

- [1] Hsu TTC, Slate FO, Sturman GM, Winter G. Microcracking of plain concrete and the shape of the stress–strain curve. *J ACI, Proceedings* 1963;60(2):209–24.
- [2] Stroeven P. Some aspects of micromechanics of concrete. PhD Thesis, Stevin Laboratory, Technological University of Delft, 1973.
- [3] Stroeven P. Application of various stereological methods to the study of the grain and the crack structure of concrete. *Journal of Microscopy* 1976;107(3):313–21.
- [4] Stroeven P. Geometric probability approach to the examination of microcracking in plain concrete. *J Mat Science* 1979;14:1141–51.
- [5] Reinhardt HW, Stroeven P. Einfluss von Schwingbreite, Belastungshöhe und Frequenz auf die Schwingfestigkeit von Beton bei niedrigen Bruchlastwechselzahlen. *Betonwerk + Fertigteil-Technik* 1978;44:498–503.
- [6] Stroeven P. Fractals and fractography in concrete technology. In: Brandt AM, Marshall IH, editors. *Brittle matrix composites 3*. London: Elsevier Appl. Science, 1991. p. 1–10.
- [7] Carpinteri A, Chiaia B, Nemati KM. Complex fracture energy dissipation in concrete under different loading conditions. *Mechanics of Materials* 1997;26(2):93–108.
- [8] Fredrich JT, Menendez B, Wang TF. Imaging the pore structure of geomaterials. *Science* 1995;268(5208):276–9.
- [9] Gertsch LS. Three-dimensional fracture network models from laboratory-scale rock samples. *International Journal of Rock Mechanics and Mining Sciences & Geomechanics Abstracts* 1995;32(1):85–91.
- [10] Montoto M, Martinez-Nistal A, Rodriguez-Ray A, Fernandez-Merayo N, Soriano P. Microfractography of granitic rocks

- under confocal scanning laser. *Journal of Microscopy-Oxford* 1995;177:138–49.
- [11] Montemagno CD, Pyrak-Nolte LJ. Porosity of natural fracture networks. *Geophysical Research Letters* 1995;22(11):1397–400.
- [12] Pyrak-Nolte LJ, Montemagno CD, Nolte DD. Volumetric imaging of aperture distributions in connected fracture networks. *Geophysical Research Letters* 1997;24(18):2343–6.
- [13] Dullien FAL. *Journal of Petroleum Technology* 1969;21:14.
- [14] Yadev GD, Dullien FAL, Chatzis I, Macdonald IF. Microscopic distribution of wetting and non-wetting phases in sandstone during immiscible displacements. In: Paper SPE 13212, 1984 SPE Annual Technical Conf. & Exhibition, Dallas, Texas, 1984.
- [15] Pyrak-Nolte LJ, Myer LR, Cook NGW, Witherspoon PA. Hydraulic and mechanical properties of natural fractures in low permeability rock. In: Herget G, Vongpaisal S, editors. *Proceedings of the Sixth International Congress on Rock Mechanics*, Montreal, Canada, August 1987. Rotterdam: A.A. Balkema, 1987. p. 225–31.
- [16] Zheng Z. Compressive stress-induced microcracks in rocks and applications to seismic anisotropy and borehole stability. PhD Thesis, Department of Material Science & Mineral Engineering, University of California, Berkeley, 1989.
- [17] Nemati KM, Monteiro PJM, Cook NGW. A new method for studying stress-induced microcracks in concrete. *American Society of Civil Engineers, Journal of Materials in Civil Engineering* 1998;10(3):128–34.
- [18] Chang CT, Monteiro PJM, Nemati KM, Shyu K. Behavior of marble under compression. *American Society of Civil Engineers, Journal of Materials in Civil Engineering* 1996;8(3):157–70.
- [19] Underwood EE. *Quantitative stereology*. New Jersey: Addison-Wesley Publishing Company, 1968.
- [20] Stroeven P. Some aspects of micromechanics of concrete. PhD Thesis, Stevin Laboratory, Technological University of Delft, 1973.
- [21] Stroeven P. Application of various stereological methods to the study of the grain and the crack structure of concrete. *Journal of Microscopy* 1976;107(3):313–21.
- [22] Stroeven P. Morphometry of plain and fibre reinforced concrete by means of image analysis techniques. In: *Proceedings of the 2nd International Conference on Mechanical Behavior of Materials*, Boston, MA, 1976. p. 1675–9.
- [23] Stroeven P. Some mechanical effects of interface debonding in plain concrete, interfaces in cementitious composites. In: Maso JC, editor. *Proceedings of the RILEM International Conference*, Toulouse, France, 1992. p. 187–96.
- [24] Ringot E. Automatic quantification of microcracks network by stereological method of total projections in mortars and concretes. *Cement and Concrete Research* 1988;18:35–43.
- [25] Massat M, Ollivier E, Ringot E. Microscopic analysis of microcracking damage in concrete and durability. Toulouse, France: *Laboratoire Materiaux et Durabilite des Constructions (INSA-UPS)*, 1988.